J Polym Res (2007) 14:373–378
DOI 10.1007/s10965-007-9119-5

Preparation and characterization of cyclo olefin copolymer (COC)/silica nanoparticle composites by solution blending

Cheng-Fang Ou · Ming-Chieh Hsu

Received: 31 January 2007 / Accepted: 15 May 2007 / Published online: 3 July 2007

Abstract A series of organic cyclo olefin copolymer (COC)/SiO_2 nanocomposites, containing 1, 5, 10 and 15 wt% SiO_2 nanoparticles, were prepared by solution blending. The differential scanning calorimetric (DSC) analysis indicated that the glass transition temperature (T_g) of composites were higher than that of pure COC and raised significantly as the SiO_2 content increased from 1 to 15 wt %. The decomposition temperatures (Td) of composites were investigated by thermogravimetric analyzer (TGA) and showed 13 °C increase by the addition of 15 wt% SiO_2 when compared to pure COC. From the scanning electron microscopic (SEM) observation, finer size of silica was dispersed in the COC matrix without large agglomerates. The light transmittance of COC/SiO_2 composites was still higher than 85% as the SiO_2 content up to 10 wt%. The oxygen barrier property of the composite film show significant improvement when compared to pure COC.

Keywords Cyclo olefin copolymer · Composites · Morphology · Transmittance · Oxygen barrier

C.-F. Ou (✉)
Department of Chemical and Materials Engineering,
National Chin-Yi University of Technology,
Taichung County 411,
Taiwan, Republic of China
e-mail: oucf@ncit.edu.tw

M.-C. Hsu
Institute of Materials and Chemical Engineering,
National Chin-Yi Institute of Technology,
Taichung County 411,
Taiwan, Republic of China

Introduction

Cyclo olefin copolymers (COC) are amorphous or semi-crystalline thermoplastics, which are manufactured by copolymerization of cyclo olefin and olefin monomers. Typically, cyclic monomer is norbornene or a derivative of norbornene (NB), and the olefin is ethylene or propylene [1–6]. The cyclo olefin monomer can undergo addition polymerization by a suitable metallocene catalyst. In addition, the COC also possesses high transparency, high glass transition temperature (T_g) and decomposition temperature (T_d), low moisture absorption, good moisture barrier and mechanical properties. This novel polymer has a potential application in optical fiber and transparent engineering thermoplastic as well as the polycarbonate does. To increase the content of ethylene in COC to increase the higher flow rate of polymer melt, which makes COC have a thermoplastic property that can be processed by extrusion and injection molding [7–10]. The manufacture and properties of COC have been studied extensively by experimental techniques, with a focus on the improvement of manufacturing technologies [11–13]. Polymer substrate has widely used in the flat panel display industry due to their flexibility, lightweight, and high power efficiencies. However, there are some technological difficulties for the realization of a display on polymer substrate, such as lower thermal stability and higher water/oxygen permeation [14–18].

Organic–inorganic polymer nanocomposites have drawn considerable attention, in recent years, due to improvements in various properties including resistance to scratching, abrasion, heat, as well as improving mechanical properties [19, 20] and the barrier properties [21]. The silica molecules act as reinforcing agents, making the polymer hardener, giving them more mechanical properties, improving their

thermal stability, and lowering the water/oxygen permeation and the coefficient of thermal expansion (CTE). Many studies have been devoted to preparation of polymer/silica hybrid materials with organic monomers and inorganic precursors such tetraethyloxysilane (SiO_2) through in situ, acid-catalyzed sol–gel processes [22–25]. The preparation and properties of COC/SiO_2 hybrid materials have been reported in our previous research [26]. In these hybrids, the inorganic molecules and organic molecules interconnect by chemical covalent bonds, hydrogen bonds or physical interaction. Different metal oxide nanoparticles can be employed as filler, in particular SiO_2, TiO_2, ZnO and CeO_2 [27]. The silica containing nanocomposites show remarkable barrier properties to gases and moisture as well as very good resistance to staining [28–32]. Sangermano et al. [32] reported the photopolymerization of epoxy coatings containing SiO_2 nanoparticles. They found that the strong decrease on water uptake in the presence of SiO_2 makes these nanocomposites materials particularly interesting for gas-barrier coatings applications. Epoxy compounds were also used for grafting SiO_x nanoparticles with poly(phenylene sulfide) (PPS) improving its impact properties [33].

In this study, the COC/SiO_2 composites constructed by COC and inorganic SiO_2 nanoparticles were prepared by solution blending. Effect of the SiO_2 content on the thermal property, thermal stability, light transmittance, morphology, and oxygen permeability are studied by DSC, TGA, UV–VIS, SEM, and gas permeability analyzer, respectively.

Experimental

Materials

The COC copolymer was a commercial product (Arton F4520) manufactured by Japan Synthetic Rubber Co., Ltd. (JSR). The chemical structure of COC was shown as the following:

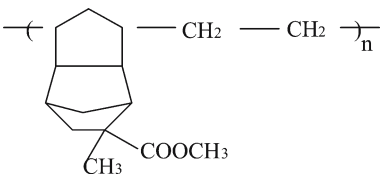

Fumed silica (SiO_2) nanoparticles used for the composite preparation, was supplied by Degussa under the trade name Aerosil 300. The average primary particle size was 7 nm, the specific surface area, 300±30 m^2/g and the SiO_2 content was >99.8%.The silica nanopowder was dried at 70°C under vacuum for 24 h before blending. Tetrahydrofuran (THF, Fisher) solvent were used as received. Deionized water used was generated from the Milli-Q plus water purification system (Millipore).

Preparation of composites

One gram COC was dissolved into 50 ml of tetrahydrofuran and stirred for 24 h. After fully dissolution, nano-sized Aerosil 300 SiO_2 powder was added to the polymer solution. Various COC/SiO_2 ratios, namely 99:1, 95:5, 90:10, and 85:15 (*w*/*w*) for the mixture were stirred for 1 h at room temperature then poured into an aluminum pan, then dried at 70°C under vacuum for 48 h to form a COC/SiO_2 composite film. The polymer film without the addition of SiO_2 is taken as the control to compare the effects of filler addition to the properties of COC.

Characterization

DSC measurements were performed with TA 2010 analyzer (TA Instruments, New Castle, DE). The sample was dried at 60°C for 6 h in a vacuum oven before DSC characterization. Appropriate amount of samples (ca. 5 mg) were sealed in aluminum sample pans. DSC analyses of these hybrid materials were then conducted under a dry nitrogen atmosphere. The samples were heated first to 250°C and kept for 3 min in the hermetic cell in order to remove the thermal history. The samples were then cooled to 30°C at the rate of 20°C/min, and then a second heating was performed at the rate of 20°C/min to 250°C. The T_g results from the second heating thermograms were the average of three samples.

The thermogravimetric (TGA) analyses of the dried composites were performed with TGA 910 (DuPont Instruments, USA), under a nitrogen atmosphere at a heating rate of 20°C/min. The structural characteristics of the raw materials and composites were analyzed with Fourier transform infrared spectrophotometer (FTIR, Nicolet Avatar 320) in special range of 4,000–400 cm^{-1} with a 4 cm^{-1} resolution. The morphology of the hybrid material was obtained from scanning electron microscopic (SEM) observation using JSM-6360 (JEOL). The optical transmittance analysis was measured by the UV–Vis spectrometer (Varian Cary-100) with wavelengths ranging from 300 to 800 nm. The oxygen permeability of hybrid film was determined by using the Yanaco GTR-10 gas permeability analyzer. The thicknesses of these films are about 100 μm. The test was carried out under isothermal condition at 35°C and the pressure is 50 kPa. The permeability is usually expressed in barrer (10^{-10} cm^3 (STP) cm/s cm cmHg).

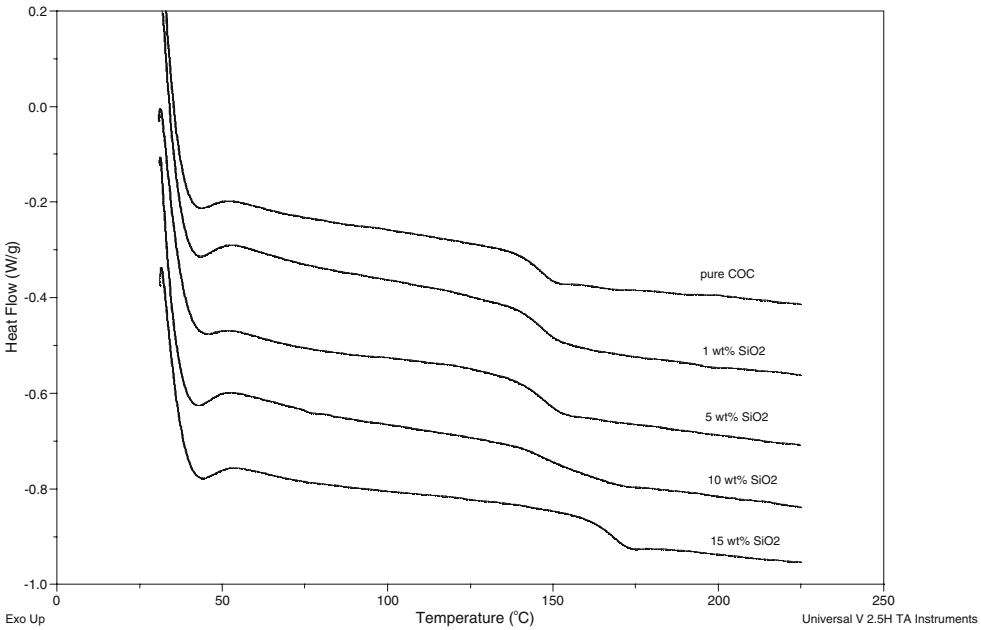

Fig. 1 DSC thermogram curves of pure COC and COC/SiO_2 composites

Results and discussions

Glass transition temperature of the composites

DSC was introduced in order to investigate the T_g of these composites. Figure 1 shows the DSC thermogram curves of pure COC and COC/SiO_2 composites. It is evident that there is a distinct single T_g located at the region from 140 to 185°C in all of the composites and the T_gs were listed in Table 1. It was found that T_g of pure COC was 146.0°C. The T_gs of the composites were higher than that of neat COC. The T_gs of these composites were raised with the increasing of the content of SiO_2 in the composites. The extreme high value of T_g was at 166.0 and 20.0°C higher than that of pure COC when the SiO_2 content increased to 15 wt%. In general, the increase on T_g is attributed to nanometric size particles that can restrict the segmental motion with a consequent increase on glass transition temperature [34, 35].

Table 1 Glass transition temperature (T_g) of COC/SiO_2 composites

Composition	T_g (°C)
Pure COC	146.0
SiO_2 1 wt%	147.0
SiO_2 5 wt%	147.4
SiO_2 10 wt%	151.7
SiO_2 15 wt%	166.0

Thermal stability of the composites

The thermal decomposition behaviors of the composites were investigated by TGA at a heating rate of 20°C/min under a nitrogen atmosphere as illustrated in Fig. 2. It was found that COC and COC/SiO_2 composites decomposed in a single stage (main degradation stage). The major weight loss of composite film is attributed to the decomposition of polymer. Pure SiO_2 does not present any abrupt decrease in weight and only a slight decrease at approximately 100°C appears due to the removal of the loss of absorbed water [36]. The data of degradation temperatures were collected from derivative thermogravimetry (DTG, not shown) curves and listed on Table 2. It was found that thermal decomposition temperatures (T_d) of COC is 472.7°C. The T_d of 1 wt% SiO_2 is about the same as that pure COC. The addition of SiO_2 from 5–15 wt% into the COC resulted in an increase of Td and increased with the increasing SiO_2 content. The composite with 15 wt% exhibits the maximum value of Td and is higher than that of pure COC by 13°C. In the case of composites, the weight retained after decomposition is dependent on the polymer content as shown in Table 2. That is, the weight residue of composites at 650°C increases with increasing SiO_2 content.

FT-IR characterization

Figure 3 shows the FT-IR spectra of composite film along with the pure COC film. The pure SiO_2 shows the characteristic bands [37, 38] at 794 cm^{-1} (symmetric Si–O–Si stretching), 1,078 cm^{-1} (asymmetric Si–O–Si stretching). The assignments of the stretching vibration bands of the

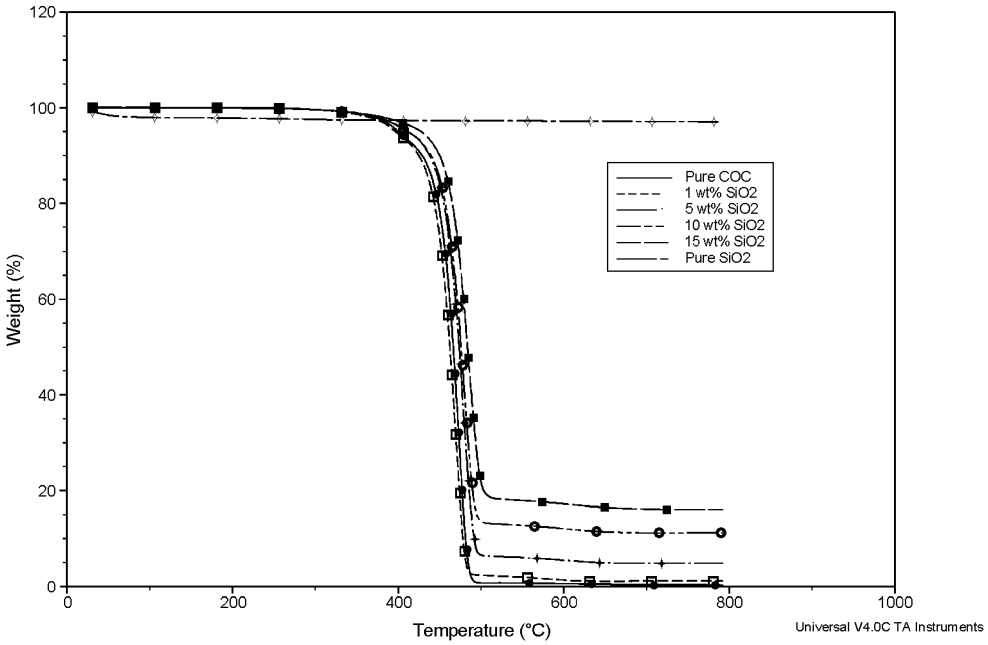

Fig. 2 TGA curves of pure COC and COC/SiO_2 composites

C=O and C–H bonds in the COC segment are at ca. 1,728 and 2,950 cm^{-1}, respectively. In the spectra of composites, both characteristic FT-IR band for SiO_2 and COC are present. The intensity of SiO_2 characteristic bands at 794 and 1,078 cm^{-1} increases with increasing SiO_2 content.

Morphology investigation

Filler dispersion and adhesion with the polymer matrix are of great importance for improving the mechanical behavior of composites. Fine control of the interface morphology of polymer nanocomposites is one of the most critical parameters to impart desired mechanical properties of such materials. In the SEM micrographs (Fig. 4), it can be seen that finer size of silica was dispersed in the COC matrix. In all the samples the silica particles are spherical in shape, with a diameter depending on the silica concentration. It is also revealed that fracture resulted in a complete debonding of the silica nanoparticles from the surrounding COC matrix, since the surfaces left were rather smooth. This is a probable indication of poor adhesion between the two phases, which resulted in the particle dispersion into the COC matrix not being homogenous.

For samples, the silica sizes detected by SEM were found to range between 40 and 300 nm for SiO_2 content from 1 to 15 wt%. Finer size of silica was dispersed in the COC matrix the sizes of SiO_2 increase a little with increasing SiO_2 content. The number of dispersed droplets in 15 wt% SiO_2 is more than that in 10 wt% SiO_2. This reveals that the number of dispersed droplets increased with the increase of SiO_2 content. These results are in good agreement with the finding of Wu et al. [39] who reported that increasing the content of SiO_2 leads to larger agglomerates.

Table 2 The TGA data of the COC/SiO_2 composites

Composition	T_d (°C)[a]	wt_R^{650} (%)[b]
Pure COC	472.7	0.3
SiO_2 1 wt%	469.2	1.3
SiO_2 5 wt%	479.2	4.6
SiO_2 10 wt%	480.3	10.9
SiO_2 15 wt%	485.7	15.7
Pure SiO_2	–	97.0

[a] Degradation temperature in this table were obtained from the peaks of the DTG data.
[b] Weight percentage of residue at 650°C.

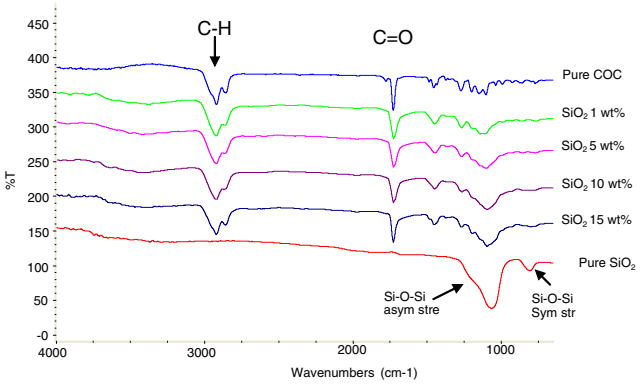

Fig. 3 FT-IR spectra of pure COC and COC/SiO_2 composites

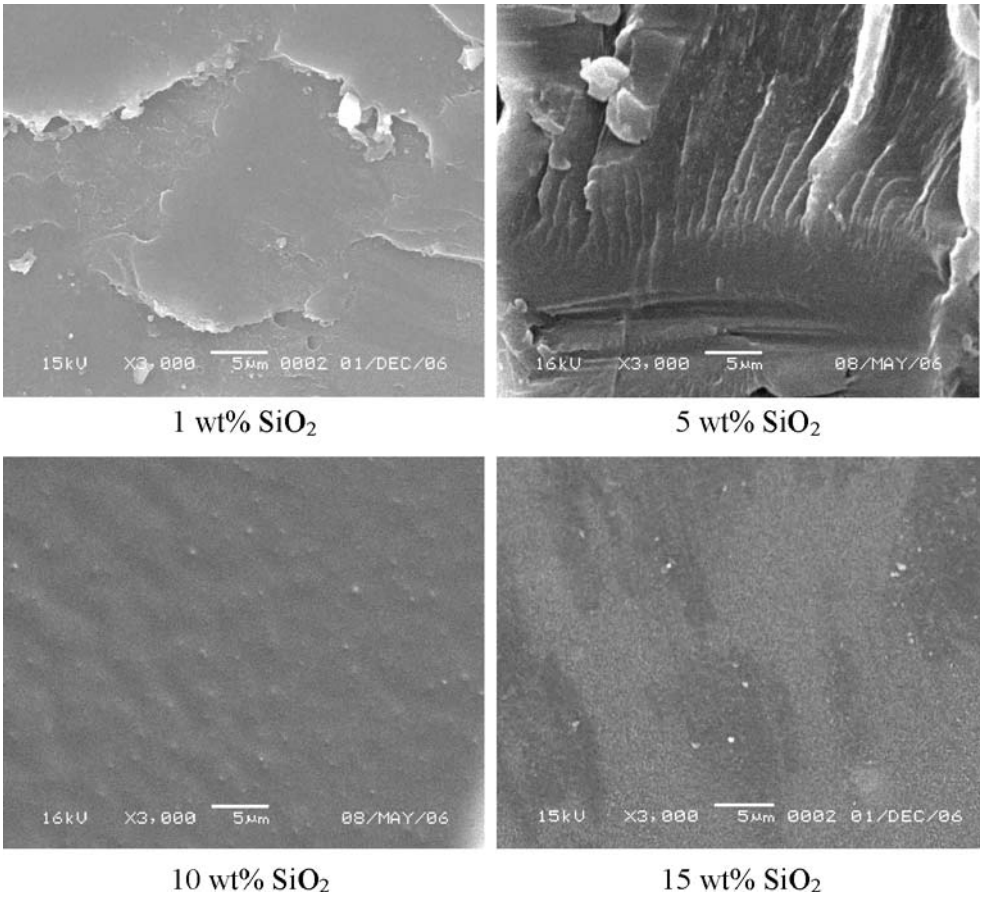

Fig. 4 SEM micrographs of the fracture surfaces of COC/SiO_2 composites

The light transmittance of the composites

The composite film was transparent at SiO_2 content levels up to 15 wt%. Figure 5 shows the UV/VIS spectra measured for various samples. The transmittance of pure COC at 550 nm was as high as 91.7%. The light transmittance of COC/SiO_2 composites were still higher than 85% at 550 nm as the SiO_2 content up to 10 wt% and a little decrease as 15 wt% SiO_2 addition. From SEM micrograph (Fig. 4), finer size of silica (40~300 nm) was dispersed in the COC matrix. These results might be the reason to exhibit the high light transmittance of COC/SiO_2 composites with SiO_2 content up to 15 wt%.

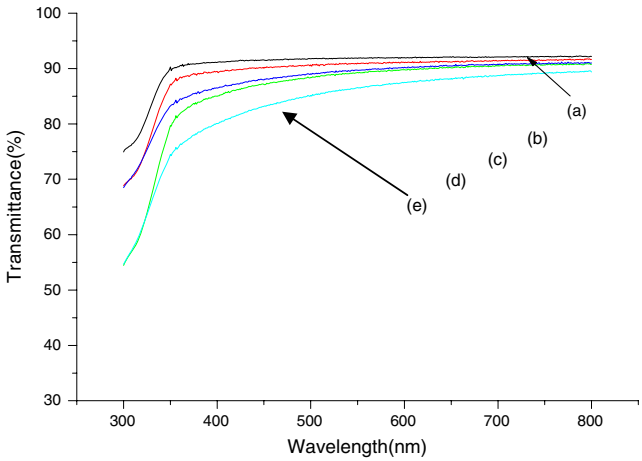

Fig. 5 UV–VIS spectra of pure COC and COC/SiO_2 composites. (*a*) Pure COC; (*b*) SiO_2 1 wt%; (*c*) SiO_2 5 wt%; (*d*) SiO_2 10 wt%; (*e*) SiO_2 15 wt%

Oxygen permeability study

Figure 6 presents the SiO_2 content dependence of oxygen permeability of COC/SiO_2 composites to pure oxygen at 35°C. The value of oxygen permeability decreases with

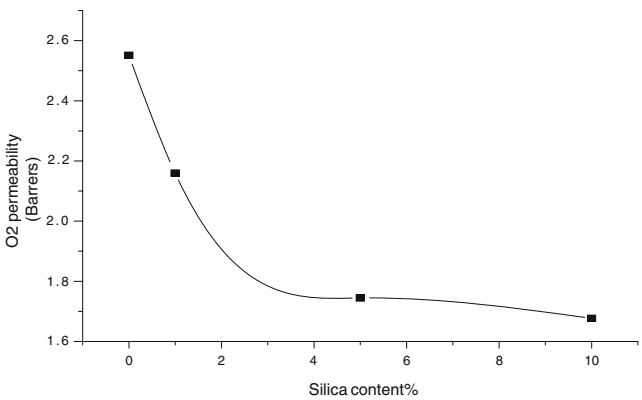

Fig. 6 Oxygen permeability of pure COC and COC/SiO_2 composites

increasing the content of SiO_2. Oxygen permeability of the pure COC and COC/SiO_2 composites are 2.55, 2.17, 1.75 and 1.50 barrers for COC, 1, 5 and 10 wt% SiO_2 composites. In the 5 wt% SiO_2, there is a significant decrease by 31% in the oxygen permeability, indicating a significantly improved oxygen-barrier property of the COC. The reduction of oxygen permeability is further decreased with increasing the content of SiO_2 to 10 wt%. The reduction of permeability arises from the longer diffusive path that the pentrants must travel in the presence of the nanoparticle.

Conclusions

In this study, it was found that the COC/SiO_2 composites exhibited the higher Tg than that of pure COC and raised as the SiO_2 content increased. The Td of COC/SiO_2 composites showed 13°C increase by the addition of 15 wt% SiO_2 when compared to pure COC. From SEM observation, finer size of silica was dispersed in the COC matrix. The light transmittance of COC/SiO_2 composites was still higher than 85% at 550 nm as the SiO_2 content up to 10 wt % and satisfied the need for optical or other applications. The oxygen barrier property of the hybrid film show significant improvement when compared to pure COC.

Acknowledgements The author would like to thank the National Science Council of the Republic of China for financially supporting this research under contract no. NSC94-2216-E-167-002.

References

1. Marathe S, Mohandas YP, Sivaram S (1995) Maromolecules 28:7318
2. Marathe S, Sivaram S (1994) Macromolecules 27:1083
3. Harrington BA, Crowther DJ (1998) J Mol Catal A 128:79
4. Kaminsky W (1999) Papra Rev Reports 10:28
5. Yeh JM, Weng CJ, Huang KY, Huang HY, Yu YH (2004) J Appl Polym Sci 94:400
6. Huang WJ, Chang FC (2003) J Polym Res 10:195
7. Kaminsky W, Bark A, Arndt M (1991) Macromol Chem Macromol Symp 47:83
8. Kaminsky W, Bark A (1992) Polym Int 28:251
9. Herfert N, Montag P, Fink G (1993) Macromol Chem 194:3167
10. Kaminsky W (1996) Macromol Chem Phys 197:3907
11. Alt FP, Heitz W (1998) Acta Polym 49:477
12. Ruchatz D, Fink G (1998) Macromolecules 31:4681
13. Kaminsky W (1994) Catal Today 20:257
14. Burrows PE, Graff GL, Gross ME, Martin PM, Shi MK, Hal IM, Mast E, Bonham C, Bennett W, Sullivan MB (2001) Display 22:65
15. Kloppel M, Kriegeis W, Meyer BK, Scharmann A, Daube C, Stollenberg J, Tube J (2000) Thin Solid Films 365:139
16. Fahland M, Karlsson P, Charton C (2001) Thin Solid Films 392:334
17. Lee MJ, Judge CP, Wright SW (2000) Solid-State Electron 44:1431
18. Henry BM, Erlat AG, McGuigan A, Grovenor CRM, Briggs GAD, Tsukahara Y, Miyamoto T, Niijima T (2001) Thin Solid Films 382:194
19. Hajji P, David L, Gerard JF, Pascault JP, Vigier G (1999) J Polym Sci Polym Phys 37:3172
20. Cho JD, Ju HT, Honh JW (2005) J Polym Sci Polym Chem 43:658
21. Huang CH, Wu JS, Huang CC, Lin LS (2004) J Polym Res 11:75
22. Weetall HH, Robertson B, Cullin D, Brown J, Walch M (1993) Biochim Biophys Acta 1142:211
23. Reetz MT, Zonta A, Simpelkamp J (1996) Biotechnol Bioeng 49:527
24. Park SH, Lee SB, Ryu DDY (1981) Biotechnol Bioeng 23:2591
25. Chang CC, Wei KH, Chang YL, Chen WC (2003) J Polym Res 10:1
26. OU CF, Hsu MC (2007) J Appl Polym Sci 104:2542
27. Reck E, Seymour S (2002) Macromol Symp 707:187
28. Borup B, Edelmann R, Mehnert R (2003) Eur Coat J 6:21
29. Atsushi B, Toshihiko T, Yuichi E, Takashi U (1997) Proc RadTech Sia, Yokohama, Japan, p 522
30. Zhou S, Wu L, Sun J (2002) Prog Org Coat 45:33
31. Bikiaris DN, Vassiliou A, Pavlidou E, Karayannidis GP (2005) Eur Polym J 41:1965
32. Sangermano M, Malucelli G, Amerio E, Priola A, Billi E, Rizza G (2005) Prog Org Coat 54:134
33. Lu D, Mai YW, Li RK, Ye L (2003) Macromol Mater Eng 288:693
34. Chan CK, Chu IM, Lee W, Chin WK (2001) Macromol Chem Phys 202:911
35. Chan CK, Chu IM, OU CF, Lin YW (2004) Mater Lett 58:2243
36. Duran A, Serna C, Fornes V, Navarro JMF (1986) J Non-Cryst Solids 82:69
37. Guglielmi M, Brusatin G, Facchin G, Gleria MJ (1996) Mater Res 11:2029
38. Bertoluzza A, Fagnano C, Gottardi V, Guglielmi M (1982) J Non-Cryst Solids 48:117
39. Wu CL, Zhang MQ, Rong MZ, Friedrich K (2002) Compos Sci Technol 62:1327